Quaternary International 357 (2015) 70–81

Contents lists available at ScienceDirect

Quaternary International

journal homepage: www.elsevier.com/locate/quaint

Late-glacial to Holocene aeolian deposition in northeastern Europe – The timing of sedimentation at the Iisaku site (NE Estonia)

Edyta Kalińska-Nartiša [a, *], Māris Nartišs [b], Christine Thiel [c, d, e], Jan–Pieter Buylaert [c, d], Andrew Sean Murray [d]

[a] Institute of Ecology and Earth Sciences, Department of Geology, Faculty of Science, University of Tartu, Ravila Str. 14A, Tartu EE50411, Estonia
[b] Faculty of Geography and Earth Sciences, University of Latvia, Alberta Str. 10, Riga LV1586, Latvia
[c] Centre for Nuclear Technologies (Nutech), Technical University of Denmark, Risø Campus, Frederiksborgvej 399, 4000 Roskilde, Denmark
[d] Nordic Laboratory for Luminescence Dating, Department of Geosciences, Aarhus University, Risø Campus, Frederiksborgvej 399, 4000 Roskilde, Denmark
[e] Leibniz Institute for Applied Geophysics (LIAG), Section S3: Geochronology and Isotope Hydrology, Stilleweg 2, 30655 Hannover, Germany

ARTICLE INFO

Article history:
Available online 6 October 2014

Keywords:
Optically stimulated luminescence dating
Sedimentary features
Late-glacial
Holocene
Inland dunes

ABSTRACT

The Late-glacial and Holocene aeolian inland dune complex at Iisaku (NE Estonia) has been investigated using an accurate and detailed compilation of the sedimentary properties and chronological framework. The quartz grains forming the dunes are very variable, reflecting aeolian, weathering, and periglacial conditions, both prior and after deposition. Although the morphological forms and the sedimentary record point to a dune-like environment, the transport record reflects either a short transport time or/and distance, and a contribution from neighbouring sedimentary environments.

Dune development in the area was strongly controlled by the formation of the Baltic Ice Lake (BIL) in front of the retreating glacier. Luminescence ages from the aeolian complex suggest continuous deposition between 13.3 ± 1.2 to 10.5 ± 0.7 ka. However, the chronology of sand deposition also suggests phases in this aeolian activity: (1) at 13.3 ± 1.2 ka and onwards, possibly correlated with the existence of an island separating the BIL and Peipsi Lake, (2) between 12.7 ± 0.8 – 12.5 ± 0.8 ka representing the Younger Dryas cold reversal, (3) between 11.5 ± 0.7 – 10.9 ± 0.8 ka indicating that aeolian deposition continued over the Younger Dryas/Holocene boundary, and (4) early Holocene sand–drift at 10.5 ± 0.7 ka.

1. Introduction

The Late-glacial–Holocene transition is characterised by a changing climate, where the temperature changed abruptly several times towards both cooler and warmer conditions (Rasmussen et al., 2006). The climatic fluctuations of the Late-glacial resulted in varying intensities of aeolian activity and vegetation growth. Alternation of phases of widespread aeolian deposition and stabilisation marked by soil formation have been found (Derese et al., 2009). The Late-glacial stratigraphic subdivision of aeolian sediments have been recognised and correlated in large parts of northwest (i.e. Kasse, 1997, 2002; Koster, 2005; Kasse et al., 2007; Vandenberghe et al., 2013) and Central Europe (i.e. Konecka-Betley and Janowska, 1976; Kaiser et al., 2009; Jankowski, 2012). Until now, no attempt has been made to directly constrain aeolian activity in time and space in Estonia, even though inland aeolian sediments are widely distributed within the basins of Lake Peipsi (Raukas, 1999) and Lake Võrtsjärv, as well as in the Hargla depression in southern Estonia. This is perhaps because these sediments tend to be sterile and do not usually contain sufficient organic material for radiocarbon dating (traditionally the technique of choice for this age range). Nor have any palaeopedological marker horizons, such as are noted in Central Europe (Kaiser et al., 2009), been established. However, due to the unique geological Late-glacial development in Estonia considerable effort has been put into setting up general chronological frameworks (Kalm, 2006), e.g. varve chronologies (Hang, 2003; Talviste et al., 2012; Hang and Kohv, 2013), beryllium dating (Rinterknecht et al., 2006), and relative dating using the palaeobotanical record (Kihno et al., 2011; Amon et al., 2012; Veski et al., 2012; Laumets et al., 2014). There are studies compiling ages for this area (Kalm et al., 2011; Lasberg and Kalm, 2013); these include ages from one very early luminescence

* Corresponding author.
E-mail address: edyta.kalinska@ut.ee (E. Kalińska-Nartiša).

http://dx.doi.org/10.1016/j.quaint.2014.08.039
1040-6182/

study (Raukas and Hüüt, 1988). Luminescence dating aims to determine the time of last exposure of a mineral grain to daylight. Thus a luminescence age usually refers to the time of sediment deposition, and the technique is ideally suited to the direct dating of aeolian activity. Previous attempts to date inland aeolian sediments of Estonia have been performed in the Iisaku area (NE Estonia) and they gave very inconclusive results (Raukas and Hüüt, 1988). The specific palaeogeographical development with a transition from glacial to glaciolacustrine and then to aeolian environment, the limited existing chronology, and the availability of fresh outcrops make the Iisaku area ideal for a new detailed study of Estonian inland dunes.

Here, we first characterise the aeolian sediments with respect to their textural features such as grain-size distributions, rounding of the quartz grains and surface character, and the light mineral content, this provides a better understanding of the origin of the sediment and the transport mechanism. In addition, several samples are dated using the latest luminescence techniques to constrain the aeolian activity in time. This combination of sedimentary studies and chronology leads to detailed insight into the depositional history of this area.

2. Geological setting and age constraints

North of Lake Peipsi (NE Estonia), in the vicinity of Iisaku, moraine ridges and kames underly a dune field showing a significant relief (Fig. 1). This relatively continuous group of dunes covers an area of about 50 km^2, up to 15–20 m in height (Raukas, 2011) and an elevation ranging from *c.* 45–55 m a.s.l. The orientations of parabolic and transverse dunes reveal a westerly-northwesterly palaeo-wind direction (Zeeberg, 1998). According to Raukas (2011), a single parabolic hill is 0.8–2.7 km in length and *c.* 50–100 m in width. Both the morphology and direction of the dunes indicate a dependence on glacial topography (Raukas, 2011). Areas located at lower elevation have been covered by organic sediments (Fig. 1A).

All deposits investigated here directly overlie the glaciolacustrine sediments of the glacial Lake Peipsi, which correlates with the Pandivere ice marginal zone of the Late Weichselian glaciation (Hang, 2003; Kalm et al., 2011). The minimum age of the Pandivere belt is indirectly supported by AMS radiocarbon (^{14}C) dates of 14,450 ± 240 cal. BP (Kihno et al., 2011) and 13,900 ± 80 cal. BP (Amon et al., 2012). A varve chronology points to the stagnation of the ice margin at the Pandivere-Neva line to ca. 13.9 to 13.7 ka in western Estonia (Hang et al., 2011), and ca. 13.5 to 13.1 ka in northeastern Estonia and in the vicinity of Lake Ladoga (Saarnisto and Saarinen, 2001; Hang, 2003). The most recent study (Vassiljev and Saarse, 2013) points to development of the A_1 phase of the BIL in front of the Pandivere ice-marginal during 13.8–14.0ka.

3. Sedimentary analysis

A total of forty-nine samples for textural feature analysis, 400–800 g each, were collected from four Iisaku locations: seventeen from the Iisaku 1 profile, twenty nine from the Iisaku 2 profiles (A, B, C, D and E), two from Iisaku 3 profile and one from the Iisaku 4 profile located within the glaciofluvial channel of the Iisaku moraine formation (Fig. 1A and B). The samples for textural features analysis were taken at 10–40 cm intervals. Directly adjacent to some of the textural samples, luminescence samples were also collected (see section 4). The lithofacies of the sediments were distinguished and described by Miall's (1978, 1977) code with the modifications proposed by Zieliński and Pisarska-Jamroży (2012). The direction of structural elements was measured for the Iisaku 3 profile, and plotted on a rose diagram, where N = population, and VM = vector mean (°) (see Fig. 2, profile Iisaku 3).

In addition to the textural analysis, grain-size analyses were performed on a total of ninety samples from the four Iisaku locations. About 200 g of each sample were dry-sieved for 20 min according to the recommendation of Syvitski (1991) and Mycielska-Dowgiałło (2007) using the sieve sizes of 1.0, 0.8, 0.5, 0.315, 0.25, 0.2, 0.125, 0.1 and 0.063 mm. The individual sieve fractions were subsequently weighed with a precision of ±0.001 g. The Folk and Ward (1957) logarithmic graphic method provided in the customised version of the R package "rysgran" (Gilbert et al., 2012) was applied to calculated the mean grain size (Mz), the sorting (σ_1) and the skewness (Sk).

The effects of wind and water are best visible in grains ~0.7 mm in diameter (Cailleux, 1952; Kotilainen, 2004). However, some researchers found the strongest aeolian abrasion in the fraction 0.8–1.0 mm (Pernarowski, 1962; Mycielska-Dowgiałło and Dzierwa, 2003; Mycielska-Dowgiałło and Woronko, 2004). A different degree of rounding within the 0.5–0.8 and 0.8–1.0 mm fraction may point to changes in transportation (Mycielska-Dowgiałło and Dzierwa, 2003). Therefore, the two sand fractions: 0.5–0.8 and 0.8–1.0 mm were separated by sieving and repeatedly washed thoroughly with water to remove any remnants of clay or

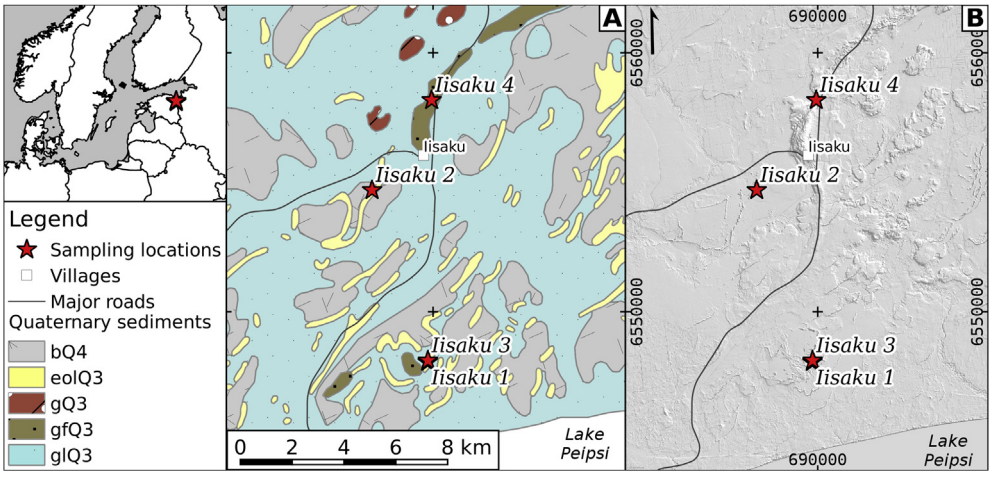

Fig. 1. Location of the investigated sites and their surrounding: A – the Quaternary sediment cover (according to Mardla, 1967); B – LiDAR elevation model (Estonian Land Board, 2013). Quaternary sediments: bQ4 – peats; eolQ3 – aeolian sands; gQ3 – glacial sediments; gfQ3 – glaciofluvial sands and gravels; glQ3 – glaciolacustrine sands.

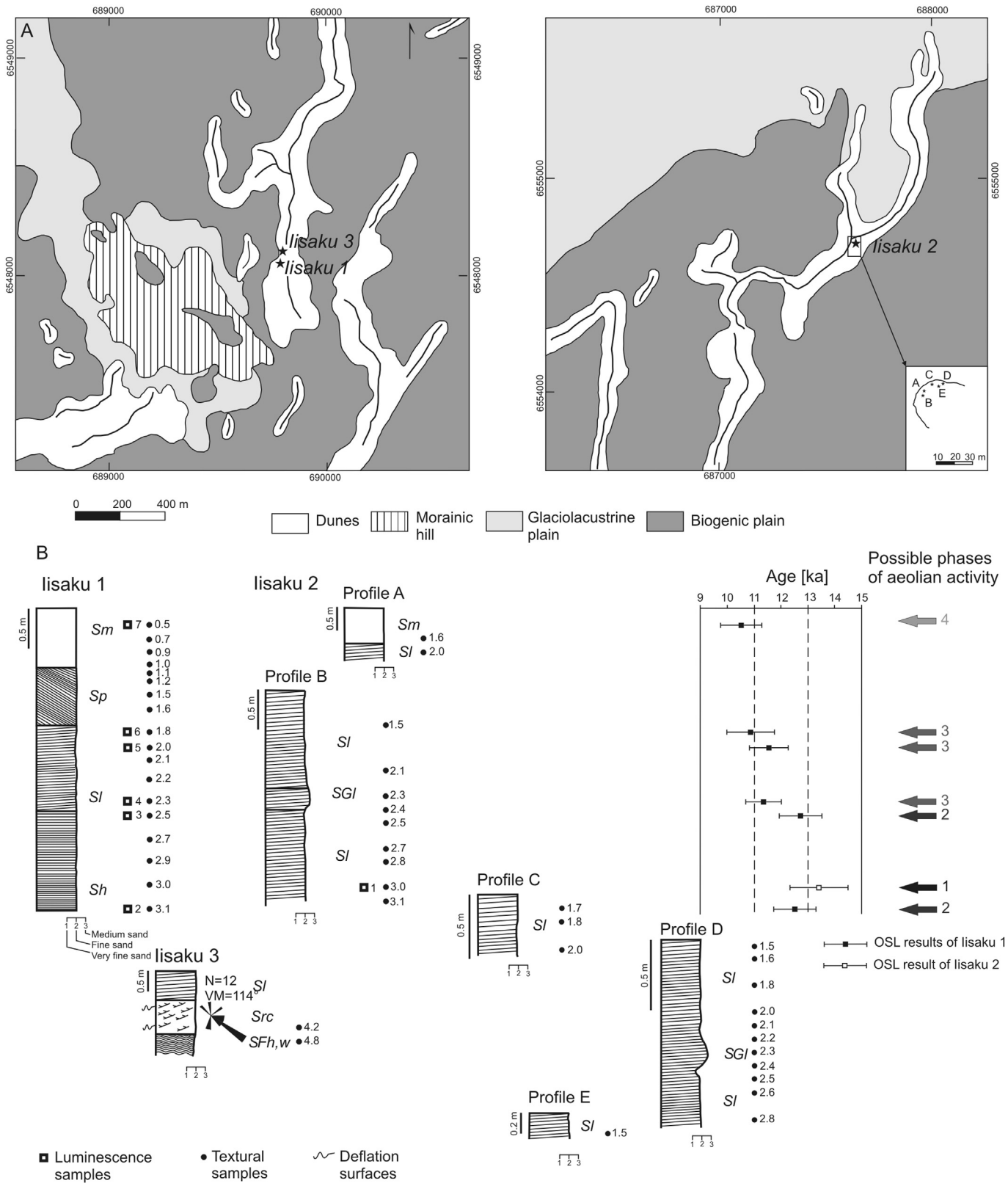

Fig. 2. A – Detailed geomorphological situation of the investigated sites. B – Logs of the sedimentary successions and luminescence ages for the investigated sites. Lithofacies symbols of sediments in profiles were distinguished by Miall's (1978, 1977) code with the modifications proposed by Zieliński and Pisarska-Jamroży (2012). The approximate spatial distribution of profiles was kept.

iron oxide coating. Under the binocular microscope with 50-× magnification rounding and surface mattness classes were determined for about 120–150 randomly selected quartz grains.

The classification of grain shape following Cailleux (1942) (modified by Mycielska-Dowgiałło and Woronko, 1998) was applied. The analysis further included assessment of grains rounding using Krumbein's (1941) scale. Seven groups of grains were determined in both sand fractions (0.5–0.8 and 0.8–1.0 mm), providing an insight into the sedimentary history of the sediment (Woronko and Hoch, 2011; Woronko, 2012a, 2012b; Woronko et al., 2013): (1) RM = aeolian well–rounded frosted (Krumbein roundness 0.7–0.9), where the high degree of rounding is an effect of long-lasting abrasion during transport in saltation (Woronko and Pochocka-Szwarc, 2013), (2) EM/RM = intermediate aeolian partially-rounded frosted (Krumbein roundness 0.3–0.6), (3) EL = high-energy aqueous environment, well-rounded shiny (Krumbein roundness 0.7–0.9), where the high degree of rounding points at long-term chemical weathering and abrasion on the grain surfaces (Woronko and Pochocka-Szwarc, 2013), (4) EL/EM = intermediate high-energy aqueous environment, partially rounded shiny (Krumbein roundness 0.3–0.6), (5) C = broken with at least 30% of the original grain surface, and (6) NU/L = fresh, non-abraded (Krumbein roundness 0.1–0.2), and (7) NU/M = outwardly frosted/matt with sharp edges without any effect of transport; a similar group has been described by Bull and Morgan (2007) and Ritchot and Cailleux (1971).

In addition, the number of quartz and feldspars grains of ~200 randomly selected grains was determined. Among the light minerals in the sand fraction (in this case 0.8–1.0 mm), quartz and feldspars are considered as particularly relevant for palaeoenvironmental analysis due to their different resistance to mechanical abrasion (Mycielska-Dowgiałło and Woronko, 2004).

4. Luminescence dating

4.1. Earlier luminescence ages from the Iisaku area

The first and, until now, only attempt to date the aeolian sequences in the Iisaku area was carried out by Raukas and Hüüt (1988) using both thermoluminescence (TL) and infrared optically stimulated luminescence (IRSL). Nine samples from three sedimentary sections, two to the south and one to the west of the town of Iisaku, resulted in an age range of between 13.6 ± 1.5 and 3.0 ± 0.5 ka (Raukas and Hüüt, 1988); in two of the profiles an age-depth inversion was observed. Both the youngest and the oldest ages were considered unreliable (Raukas and Hüüt, 1988; Raukas, 1999) and only the range between 4.0 ± 0.5 to 7.1 ± 0.7 ka was considered to point to different phases of aeolian activity in this area. Raukas (1999) has concluded that the dating of aeolian deposits is extremely difficult due to their repeated re-deposition. The results obtained by infrared optically stimulated luminescence from the upper part of a recently deposited dune and a palaeodune from the northern coast of Lake Peipsi were considered more reliable (Raukas and Hüüt, 1988). These gave ages between 1.0 ± 0.2 and 0.5 ± 0.5 ka for the modern samples, and 8.0 ± 0.3 ka for the palaeodune. Hence, the results from both TL and IRSL are in generally good agreement. Nevertheless, the samples suffer from a large error range (20–100%), and the effect of anomalous fading in feldspar was not considered; this tends to result in age underestimation.

4.2. Luminescence dating: this study

Two sections were sampled, to the south and west of the town of Iisaku (Iisaku 1 and Iiasku 2 profiles, respectively; cf. Figs. 1 and 2A,B). In total, seven samples (six from the Iisaku 1, and one from Iisaku 2 site) were collected for luminescence dating. At the Iisaku 1 profile, samples were taken with relatively close spacing (between 20 and 130 cm). In contrast, the Iisaku 2 site, was documented only by a single sample located within the middle part of the leeward slope of a parabolic dune. No lithostratigraphic horizons could be identified, and so samples were taken according to depth. Samples were collected in 0.5 m long opaque PCV tubes that were hammered into the sediment. The tubes were dug out and immediately capped to minimise light exposure.

In the laboratory the sample tubes were opened under subdued red light conditions. The sediment at each end of the tubes, which might have been exposed to daylight while sampling, was retained to determine the dose rate and the water content. The dose rate samples were dried, ashed (24 h at 450 °C), ground and thus homogenised, and subsequently cast in wax in a fixed geometry. The casts were stored for at least three weeks prior to radionuclide concentration measurements using a high-resolution gamma spectrometer (Murray et al., 1987). These radionuclide concentrations (Table 1) have been converted into beta and gamma dose rates following Olley et al. (1996). For all samples except sample Iisaku 1 3,1 (VI) (ID 123076; Table 1) a life-time burial water content of 7% was used; this is the water content observed in the dune sediments. Sample Iisaku 1 3,1 (VI) showed a different sedimentary structure, and it was evident in the field that it must have been at least partly saturated during burial. Accordingly, the average of the field and saturated water contents (23%, with respect to dry weight) was used for this sample. To allow for changes in water content over time, an absolute uncertainty of 4% was incorporated in the calculation. The resulting total dose rates are listed in Table 1.

Table 1
Summary of radionuclide concentrations, water content, dose rates (D_r), equivalent doses (D_e) and ages. n = number of aliquots measured to obtain average D_e's; s.e. = standard error.

Field ID	Laboratory ID	^{226}Ra ± s.e. (Bq/kg)	^{232}Th ± s.e. (Bq/kg)	^{4}K ± s.e. (Bq/kg)	Total dose rate ± s.e. (Gy/ka)	n	D_e ± s.e. (Gy)	Age ± s.e.(ka)
Iisaku 2 3,0 (I)	123071	14.48 ± 0.35	15.76 ± 0.40	409 ± 8	1.83 ± 0.08	10	24.3 ± 1.7	13.3 ± 1.2
Iisaku 1 2,0 (II)	123072	12.33 ± 0.36	14.76 ± 0.36	475 ± 11	2.01 ± 0.09	13	23.0 ± 0.9	11.5 ± 0.7
Iisaku 1 1,8 (III)	123073	13.02 ± 0.56	13.05 ± 0.60	496 ± 12	2.07 ± 0.10	12	22.5 ± 1.3	10.9 ± 0.8
Iisaku 1 2,5 (IV)	123074	12.59 ± 0.47	12.83 ± 0.51	472 ± 11	1.97 ± 0.09	11	25.0 ± 0.9	12.7 ± 0.8
Iisaku 1 0,5 (V)	123075	13.84 ± 0.41	17.35 ± 0.48	510 ± 10	2.24 ± 0.10	12	23.6 ± 1.1	10.5 ± 0.7
Iisaku 1 3,1 (VI)	123076	17.71 ± 0.49	22.44 ± 0.51	550 ± 13	2.09 ± 0.08	9	26.0 ± 1.2	12.5 ± 0.8
Iisaku 1 2,3 (VII)	123077	11.91 ± 0.42	13.63 ± 0.49	520 ± 12	2.16 ± 0.10	10	24.3 ± 0.9	11.3 ± 0.7

The inner parts of the tube samples were prepared for OSL measurements. The 180–250 μm quartz fraction was extracted using standard laboratory procedures, i.e. wet sieving, 10% HCl for 1 h to remove carbonates, 10% H_2O_2 for 1 h to remove organic

material, 10% HF to clean the outer surface of the grains, and aqueous heavy liquid separation ($\rho = 2.58$ g cm^{-3}) to separate potassium feldspar. Finally the quartz-rich extracts (>2.58 g cm^{-3}) were etched with 40% HF for 1 h to remove any remaining feldspar and the outer alpha-irradiated layer. After drying, the samples were re-sieved.

To test the purity of the quartz, three aliquots of each sample were measured following Duller (2003). The test showed that all samples were contaminated by feldspar. As a result, the quartz extracts were re-etched (40% HF, 1 h) at least once more. Even after this aggressive treatment, no pure quartz signal could be obtained, implying that the quartz contains feldspar inclusions. In order to obtain a purer quartz signal, a post-IR pulsed blue OSL (Denby et al., 2006; Thomsen et al., 2008) single aliquot regenerative dose protocol (SAR; Murray and Wintle, 2000) was applied, using an automated Risø TL/OSL reader (model DA-20; Thomsen et al., 2006). Both infrared (IR) and blue light emitting diodes (LEDs) were used for stimulation, and the luminescence was detected through a Hoya U-340 filter (i.e. ultraviolet part of the light spectra).

Our SAR protocol involved a preheat of 260 °C (10 s), and after a subsequent IR stimulation at 50 °C (100 s), pulsed blue stimulation at 125 °C (100 s) was applied, with an on- and off-time each of 50 μs; data were collected during the off-periods. The response to a test dose of ~25 Gy was measured in the same way after preheating to 220 °C. At the end of each SAR cycle, a high-temperature illumination (blue light) was employed to minimise any signal carry-over. The initial 0.4 s of the decay curve less a background of the subsequent 2 s were used to construct the growth curves which were fitted with a single exponential function. At least nine aliquots were measured per sample (see Table 1); these all passed standard quality tests (cf. Wintle and Murray, 2006). The OSL-IR depletion ratio (Duller, 2003) was measured for each aliquot, and this resulted in an average of 0.98 ± 0.03 ($n = 21$), showing that on average any feldspar contribution was successfully removed using pulsed OSL.

To test whether the measurement protocol can accurately measure a dose given prior to heating, a dose recovery test was conducted on all samples. Three aliquots each were bleached (blue LEDs) for 100 s twice with a pause of 10,000 s in between the two bleaching steps. A dose similar to the natural dose was then given to each of the aliquots which were subsequently measured as described above. The average measured to given ratio was 1.07 ± 0.03 ($n = 19$), clearly showing the applicability of the measurement protocol to our samples. The equivalent doses for the seven samples are listed in Table 1 and are discussed in Section 6.2.

5. Results of the sediment analyses

5.1. Sedimentary features

Three genetic types of aeolian deposits could be distinguished at the Iisaku site: (1) aeolian deposits related to the windward sub-environment (Iisaku 1 and 3; Fig. 3A and C), (2) aeolian sub-environment of the lee face (Iisaku 2, Fig. 3B), and (3) coversands (the uppermost part of the Iisaku 1 profile; Fig. 3A). Moreover, the lowest accessible part of the sequence, represented by the lowest part of the Iisaku 1 and 3 profiles, could be related to the glaciolacustrine environment of the underlying sediments, being composed of horizontal and climbing translatent stratificated (*Src*) sands intercalated with silt or silty sands with horizontal and wavy lamination (*SFh,w*) (Fig. 3D and E). The middle and upper part of the Iisaku 1 profile show tabular cross-stratification (*Sp*) and low-angle inclined stratification (*Sl*) (Fig. 3F). In some parts of the Iisaku 2 profile (profiles B and D; Fig. 3G) as well as in the top of the Iisaku 3 profile (Fig. 3H) a climbing translatent stratification is present with an alternation of coarser and finer grained laminae. Occasionally, ~5 cm long coarse-grained lenses are present in the Iisaku 1 and 2 profiles; these can be interpreted as granule ripples (Fig. 3I). Towards the top, the coarser-to-finer stratification is less visible due to post-depositional pedogenesis. At the Iisaku 2 site the large scale inclined stratification (*Sl*) confirms the presence of the lee face sub-environment (Fig. 3J). In the uppermost part of the Iisaku 1 and 2 profiles fined-grained sand with a massive structure can be found. Some of the deflation surfaces can be seen in Fig. 3E and H.

5.2. Grain size

Most of the Iisaku profiles consists of fairly homogenous fine-grained sands with a mean (Mz) value between 1.95 and 2.76 phi (Table 2, Fig. 4). The alternation of the coarser- and finer-grained laminae and lenses is visible in some part of the profiles. The sediments show good and moderate sorting (between 0.37 and 0.89), and both negative and positive skewness with values ranging from −0.284 to 0.144.

Table 2
Folk and Ward (1957) indicators of the investigated deposits: Mz – mean, σ – standard deviation, Sk – skewness.

Profile/site		Depth [m]	Mz	Σ	Sk
Iisaku 1		0.5	2.57	0.51	−0.11
		0.7	2.57	0.45	−0.13
		0.9	2.45	0.64	−0.18
		1.0	2.72	0.43	0.00
		1.1	2.46	0.52	−0.08
		1.2	2.40	0.64	−0.22
		1.5	2.70	0.38	0.00
		1.6	2.53	0.60	−0.20
		1.8	2.47	0.50	−0.15
		2.0	2.25	0.67	−0.04
		2.1	2.47	0.58	−0.16
		2.2	2.71	0.50	0.03
		2.3	2.50	0.51	−0.11
		2.5	2.76	0.47	0.10
		2.7	2.72	0.47	0.02
		2.9	2.74	0.45	0.01
		3.0	2.56	0.61	−0.10
		3.1	2.58	0.54	−0.07
Iisaku 2	A	1.6	2.56	0.62	−0.14
		2.0	2.27	0.66	−0.01
	B	1.5	2.46	0.60	−0.14
		2.1	2.16	0.71	−0.10
		2.3	1.95	0.89	−0.01
		2.4	2.08	0.84	−0.22
		2.5	2.40	0.64	−0.21
		2.7	2.63	0.66	−0.17
		2.8	2.56	0.57	−0.15
		3.0	2.67	0.58	−0.10
		3.1	2.4	0.63	−0.18
	C	1.7	2.38	0.67	−0.18
		1.8	2.27	0.89	−0.28
		2.0	2.41	0.68	−0.18
	D	1.5	2.72	0.44	0.02
		1.6	2.50	0.50	−0.14
		1.8	2.54	0.51	−0.21
		2.0	2.53	0.44	−0.17
		2.1	2.23	0.69	−0.10
		2.2	2.42	0.59	−0.28
		2.3	1.91	0.83	−0.12
		2.4	2.54	0.43	−0.16
		2.5	2.75	0.43	0.03
		2.6	2.17	0.71	−0.12
		2.8	2.38	0.50	−0.25
	E	1.5	2.00	0.71	0.14
Iisaku 3		4.2	2.50	0.70	−0.14
		4.8	2.64	0.56	−0.07

Fig. 3. The sedimentary structures observed at the investigated sites: A, B, C – sections of the aeolian complex in Iisaku 1 (A), Iisaku 2 with A–E profiles, (B) and Iisaku 3 (C); D – horizontal and wavy sands intercalated with silts (*SFh,w)* and climbing translatent stratificated sands *(Src)* at the bottom of the Iisaku 3 profile; E – two sets of the climbing translatent stratification separated by the deflation surface at the bottom of the Iisaku 3 profile; F – tabular cross–stratification (*Sp*) and low–angle inclined stratification (*Sl*) in the middle part of the Iisaku 1 profile; G –climbing translatent stratification *(Src)* with an alternation of coarser- and finer-grained laminae within the lee–ward slope of the Iisaku 2 site; H – climbing translatent stratification *(Src)* with an alternation of coarser- and finer-grained laminae in the middle part of Iisaku 3 profile; I – granule ripples within the lee–ward slope of the Iisaku 2 site; J –large scale inclined stratification *(Sl)* within the leeward slope of the Iisaku 2 site; G –luminescence sample collection. Locations of the textural and luminescence samples are marked by dots and rectangles, respectively.

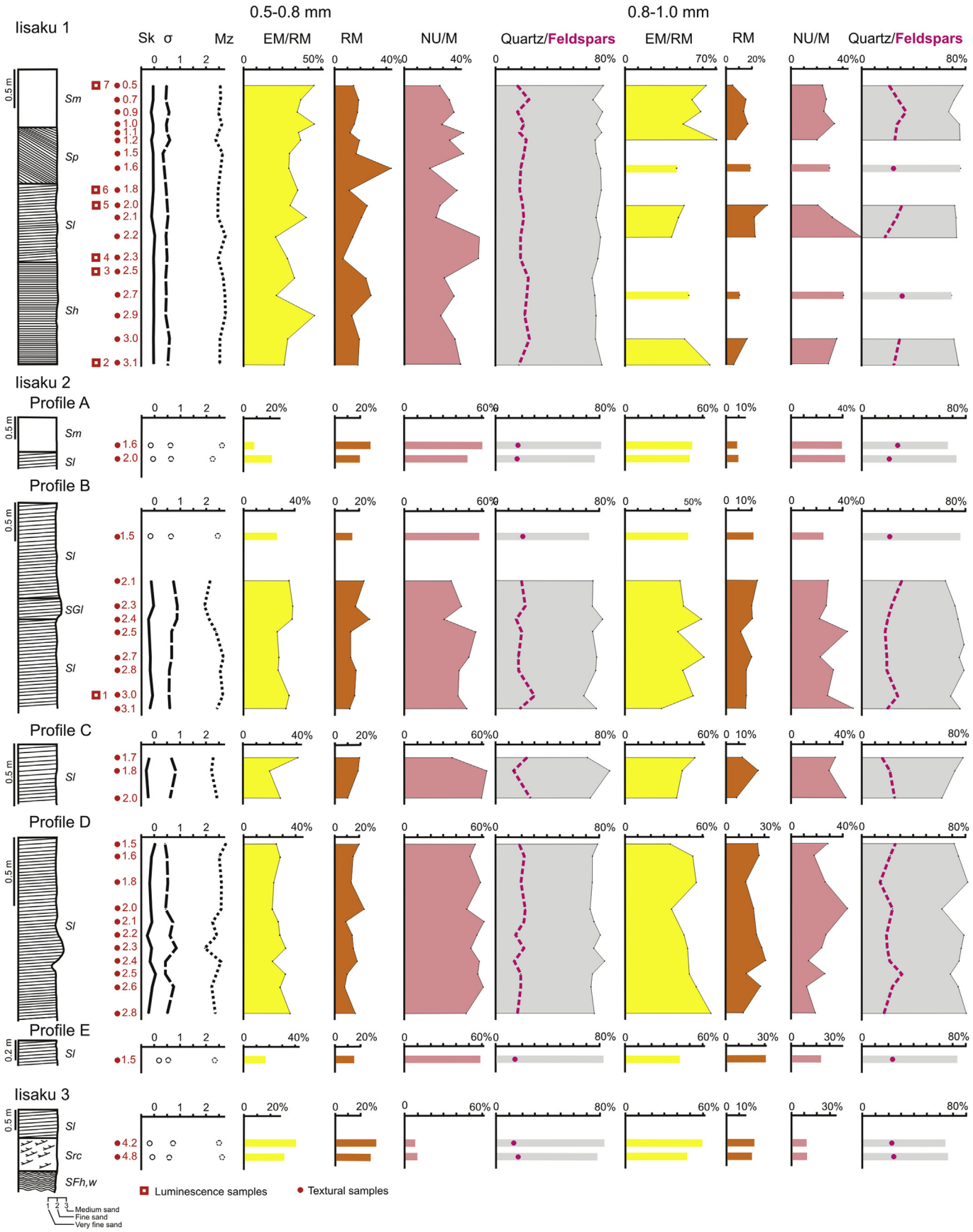

Fig. 4. Selected results of the investigation on the aeolian Iisaku complex: Mz – mean, σ – standard deviation, Sk – skewness, EM/RM – partially rounded matt quartz grains, RM – well-rounded matt quartz grains, NU/M– matt quartz grains with sharp edges. The textural and luminescence samples are marked by dots and rectangles, respectively. The OSL age of luminescence samples are: 1) 13.3 ± 1.2 ka, 2) 12.5 ± 0.8 ka, 3) 12.7 ± 0.8, 4) 11.3 ± 0.7 ka, 5) 11.5 ± 0.7 ka, 6) 10.9 ± 0.8 ka, 7) 10.5 ± 0.7 ka.

5.3. Rounding and frosting

Two types of aeolian quartz grains within the sandy fractions (0.5–0.8 and 0.8–1.0 mm) dominate the Iisaku sediments (Table 3, Fig. 4): (1) well-rounded (RM), and (2) partially rounded where the aeolian activity is only visible on the edges and corners of grains (EM/RM). The number of RM grains ranges from 6.0% to 44% (Iisaku 1 at depths of 2.3 m and 1.6 m, respectively) in the 0.5–0.8 mm fraction, and from 4.6% to 31% (Iisaku 1 at depths of 3.1 m and 2.0 m, respectively) in the coarser fraction. In addition, the EM/RM grains vary between 9.8% and 54.4% (Iisaku 2, profile A at a depth of 1.6 m, and Iisaku 1 at a depth of 0.5 m) in the finer fraction, and between 28% and 71% (Iisaku 2, profile B at a depth of 3.1 m, and Iisaku 1 at a depth 1.2 m) in the coarser fraction. The non-abraded *in situ* weathered grains (NU/M) show a wide range from 8.9 to 62% (Iisaku 3 at a depth 4.2 m, and Iisaku 2, profile C at a depth of 1.8 m, respectively). In the coarser fraction the number of others grains ranges from 10% to 44% (Iisaku 3, 4.8 m and Iisaku 2, profile B, 2.5 m, respectively). In addition, the share of broken (C) type grains is variable (0–14% in the 0.5–0.8 mm fraction, and 0%–14% in the 0.8–1.0 mm fraction, respectively); the Iisaku 3 profiles show the largest proportion of the aforementioned grains. Both the fresh (NU) and the shiny (EM/EL + EL) grains are rather rare and occur only within some parts of the profiles (i.e. Iisaku 1 at a depth of 2.0 m, or Iisaku 3 at a depth of 4.2 m) (cf. Table 3).

Table 3
Results of the rounding and frosting of quartz grains and light minerals content of the investigated deposits: 1 – aeolian–type grains (RM – well–rounded matt and EM/RM – partially rounded matt), 2 – *in situ* mechanically/chemically weathered grains – NU/M– matt quartz grains with sharp edges, 3 – fluvial–type grains – EM/EL – partially rounded shiny, 4 – postsedimentary frost weathered grains – C – cracked, 5 – glacially transformed or frost weathered grains – NU/L – shiny with sharp edges, Q – quartz, F – feldspars, C – particles of crystalline rocks. Data for Iisaku 1 partially after Kalińska and Nartišs (2014).

Site		Depth [m]	Types of grains												Mineral content					
			0.5–0.8 mm						0.8–1.0 mm						0.5–0.8 mm			0.8–1.0 mm		
			1		2	3	4	5	1		2	3	4	5						
			RM	EM/RM	NU/M	EM/EL	C	NU/L	RM	EM/RM	NU/M	EM/EL	C	NU/L	Q	F	C	Q	F	C
Iisaku 1		0.5	15.20	54.40	27.20	0.00	2.40	0.00	4.65	62.79	23.25	2.32	0.00	6.98	82.61	13.48	3.91	78.33	11.67	10.0
		0.7	18.93	43.18	34.84	0.00	3.03	0.00	15.15	51.52	27.27	3.03	3.03	0.00	74.56	19.30	6.14	71.43	28.57	0.00
		0.9	18.38	40.44	37.50	0.00	3.68	0.00	12.50	58.33	25.83	1.66	1.67	0.00	82.19	15.98	1.83	67.07	21.95	10.97
		1.0	16.67	54.17	29.17	0.00	0.00	0.00	17.24	43.1	32.76	0.00	3.45	3.45	78.51	16.11	5.37	74.07	24.70	2.47
		1.1	10.32	41.27	45.24	3.17	0.00	0.00	–	–	–	–	–	–	81.78	14.87	3.36	–	–	–
		1.2	19.83	43.10	34.49	0.00	2.59	0.00	7.37	70.53	20.00	0.00	2.10	0.00	76.92	19.84	3.24	74.23	17.03	8.73
		1.5	17.24	35.34	45.69	0.86	0.86	0.00	–	–	–	–	–	–	78.53	14.74	6.73	–	–	–
		1.6	43.75	35.16	19.53	0.00	0.78	0.78	18.18	39.39	31.82	1.51	6.06	3.03	80.72	17.49	1.79	76.92	14.29	8.79
		1.8	11.51	41.01	41.01	2.16	4.32	0.00	–	–	–	–	–	–	81.08	16.60	2.32	–	–	–
		2.0	24.22	35.94	27.34	1.56	1.56	8.59	31.13	45.28	20.75	0.94	0.94	0.94	79.30	18.06	2.64	71.94	23.74	4.32
		2.1	20.80	48.80	24.80	3.20	2.40	0.00	21.24	40.71	31.86	0.88	2.65	2.65	78.19	19.75	2.06	72.54	19.69	7.78
		2.2	13.01	24.40	57.72	2.44	2.44	0.00	9.52	23.81	57.14	0.00	9.52	0.00	80.19	15.09	4.24	81.48	14.81	3.70
		2.3	5.98	32.48	56.41	1.71	3.42	0.00	–	–	–	–	–	–	79.83	16.81	2.94	–	–	–
		2.5	24.60	39.68	30.95	3.97	0.79	0.00	–	–	–	–	–	–	74.07	21.29	4.17	–	–	–
		2.7	28.57	25.00	38.57	4.29	3.57	0.00	10.20	48.98	40.82	0.00	0.00	0.00	76.23	20.18	3.14	69.23	24.36	6.41
		2.9	12.78	54.13	27.07	1.50	4.51	0.00	–	–	–	–	–	–	77.87	18.85	3.28	–	–	–
		3.0	19.17	34.93	39.04	0.68	6.16	0.00	16.67	45.83	34.72	0.00	1.39	1.39	76.64	19.34	4.01	70.33	29.67	0.00
		3.1	19.38	31.01	42.63	3.10	3.10	0.00	5.26	65.79	28.95	0.00	0.00	0.00	81.63	13.06	5.31	74.83	19.73	5.44
Iisaku 2	A	1.6	27.27	9.85	60.61	2.28	0.00	0.00	7.25	50.72	39.13	1.45	1.45	0.00	80.36	17.41	2.23	67.35	27.55	3.70
		2.0	19.35	21.29	49.68	8.39	1.29	0.00	9.78	47.83	40.22	0.00	2.17	0.00	76.92	16.29	6.79	73.45	20.90	5.65
	B	1.5	13.53	25.56	57.89	0.00	3.01	0.00	21.05	48.24	24.56	1.75	1.75	2.63	74.24	21.83	3.93	75.86	21.38	2.76
		2.1	23.08	36.15	36.15	3.85	0.77	0.00	23.76	42.57	29.70	1.98	1.98	0.00	75.00	17.50	7.50	64.52	30.97	4.52
		2.3	12.40	41.32	42.98	0.00	3.31	0.00	14.28	45.53	27.68	0.89	3.57	8.03	74.56	21.93	3.51	71.43	22.62	5.95
		2.4	27.56	38.52	30.71	2.36	0.79	0.00	15.00	59.00	22.00	2.00	1.00	1.00	81.08	16.22	2.70	74.28	20.00	5.71
		2.5	12.98	25.95	54.96	3.82	2.29	0.00	11.63	40.70	44.19	2.32	0.00	1.16	74.24	20.09	5.68	79.75	17.79	2.45
		2.7	12.88	27.27	53.03	3.79	3.03	0.00	13.39	60.71	22.32	0.89	1.78	0.89	78.51	17.36	4.13	76.09	19.56	4.35
		2.8	17.54	28.95	42.10	2.63	8.77	0.00	15.62	44.80	32.30	4.17	3.12	0.00	77.67	17.96	4.37	79.36	19.05	1.59
		3.0	16.92	35.39	41.54	0.77	4.61	0.00	15.69	52.94	28.43	0.98	1.96	0.00	68.38	28.20	3.42	69.18	27.04	3.77
		3.1	10.64	32.62	48.23	4.25	4.25	0.00	14.00	28.00	51.00	1.00	2.00	3.00	77.63	18.26	4.11	76.09	19.56	4.35
	C	1.7	18.71	41.01	36.00	2.88	1.44	0.00	17.65	60.50	19.33	1.68	0.84	0.00	76.56	20.09	3.35	71.43	23.21	5.36
		1.8	17.81	18.49	61.64	1.37	0.68	0.00	27.72	51.48	13.86	1.00	4.95	1.00	77.62	16.89	5.48	62.07	34.48	3.45
		2.0	8.69	28.26	55.07	6.52	1.45	0.00	20.80	40.80	30.40	1.60	2.40	4.00	71.43	17.06	11.11	76.92	17.95	5.13
	D	1.5	20.00	24.28	53.57	0.71	1.43	0.00	24.10	35.18	29.63	5.56	1.85	3.70	78.34	18.43	3.23	71.60	24.69	3.70
		1.6	15.28	28.47	50.70	2.08	3.47	0.00	26.00	53.00	18.00	1.00	1.00	1.00	75.56	21.33	3.11	74.32	21.62	4.05
		1.8	12.60	22.69	58.82	4.20	1.68	0.00	14.75	55.74	26.23	1.64	1.64	0.00	75.63	19.75	4.62	81.71	13.41	4.88
		2.0	23.08	21.68	48.95	2.10	4.19	0.00	21.80	35.90	42.31	0.00	0.00	0.00	73.73	22.12	4.15	72.00	23.20	4.80
		2.1	9.49	26.28	61.31	1.46	1.46	0.00	–	–	–	–	–	–	76.00	21.60	2.40	–	–	–
		2.2	13.14	28.45	56.20	0.73	1.46	0.00	23.08	45.30	27.35	0.85	3.42	0.00	80.51	16.10	3.39	79.10	18.64	2.26
		2.3	15.69	30.72	50.98	1.96	0.65	0.00	26.90	47.90	23.53	0.00	1.70	0.00	75.89	21.43	2.68	77.78	19.44	2.78
		2.4	18.92	20.27	58.78	0.67	1.35	0.00	30.95	53.57	13.09	2.38	0.00	0.00	84.07	14.16	1.77	75.47	21.70	2.83
		2.5	10.00	30.77	56.92	2.31	0.00	0.00	15.38	50.00	26.92	0.00	1.92	3.85	75.63	18.91	5.46	67.95	30.77	1.28
		2.6	8.33	27.50	60.83	1.67	1.67	0.00	26.78	54.46	11.61	0.89	6.25	0.00	73.73	19.35	6.91	74.87	23.00	2.13
		2.8	17.09	35.90	47.01	0.00	0.00	0.00	12.50	67.04	19.32	0.00	0.00	1.14	76.58	17.58	5.84	80.36	17.86	1.78
	E	1.5	15.72	18.57	59.28	5.00	1.43	0.00	31.10	41.17	23.53	0.84	1.68	1.68	82.12	15.49	2.41	73.86	23.86	2.27
Iisaku 3		4.2	30.69	40.59	8.91	3.96	10.89	4.95	20.25	59.49	10.13	2.53	6.33	1.27	82.13	13.53	4.35	73.45	20.90	5.65
		4.8	25.00	30.83	9.17	10.0	14.17	10.0	19.28	38.96	10.39	9.09	14.29	3.90	78.53	16.75	4.19	66.27	24.10	9.64

5.4. Light minerals

The aeolian deposits show a quartz-feldspar mixture (Table 3, Fig. 4). Both high concentration of feldspars (between 13% and 28% for the 0.5–0.8 mm fraction and 12 and 34% for the 0.8–1.0 mm fraction, respectively), and particles of crystalline rocks (between 1.8–11% and 0–11% for the 0.5–0.8 and 0.8–1.0 mm fractions, respectively) were found. No vertical relationship, e.g. diminishing of the feldspar proportion near the dune surface, was observed. The more easily-winnowed micaous group minerals are in minority (>1.0%) in some parts of the studied profiles. The light mineral content of the aeolian samples correlates well with the glaciofluvial channel deposits of the Iisaku moraine formation, where the content of feldspars reaches 28% and 27% (0.5–0.8 and 0.8–1.0 mm fraction, respectively).

6. Discussion

6.1. Interpretation of sediment features and the potential source of the sediments

The overall horizontal and low-angle stratification and homogeneity points to the aeolian nature of the sediments (cf. Vandenberghe et al., 2013). Alternating bedding of silty, fine and coarser sand can be attributed to the deposition and adhesion of sediments on an alternating dry and wet depositional sand sheet/dune surface and/or seasonal changes in wind velocity (Kasse, 2002). In contrast, the sandy-silty undulating strata observed at the bottom of the Iisaku 3 profile may represent the last glaciolacustrine event within the BIL. The cyclicity of the units may be explained by a significant water level fluctuation caused by partial drainage of the still existing lake (Hanson et al., 2012). Therefore, the character of the glaciolacustrine to aeolian transition is zonal and gentle and does not resemble the rapidly changing conditions known from e.g. central Poland (Kalińska, 2012). The local deflation horizons and the occurrence of coarser-grained lenses record short deflation episodes. The absence of distinct horizons such as e.g. the 'Beuningen gravel bed' (Bateman and Van Huissteden, 1999; Kasse et al., 2007; Vandenberghe et al., 2013) may reflect wetter local conditions which have been also been noted in southern Poland and northern Ukraine (Zieliński et al., 2014). Similar characteristics have been recognised (Vandenberghe et al., 2013) within a large part of the aeolian unit 'Older Coversand II' in The Netherlands, indicating deposition in a relatively warmer climate without permafrost.

The roundness analysis of the quartz sand grains and their surface character revealed a predominance of matt surfaces with various degrees of rounding. This suggests a predominance of aeolian factors (Mycielska-Dowgiałło and Woronko, 2004; Velichko et al., 2011; Woronko, 2012a). Nevertheless, for most of the samples examined here, traces of aeolian action are only recognised easily at the corners and edges of the grains. This suggests either a relatively short period of abrasion and/or short transport distance (Mycielska-Dowgiałło, 1993; Narayana et al., 2010). According to Mycielska-Dowgiałło (1993), sediments are only dominated by grains of the EM/RM type if the period of wind activity lasts some hundreds of years. The slight increase in long-duration grain abrasion (RM) observed e.g. in the Iisaku 1 profile at a depth of 1.6 m, probably reflects the synchronous occurrence of intense aeolian processes. Grains of the RM group grains are not only perfectly spherical, but also diverse in shape. The latter could point to various agents and incomplete transformation by low wind-speeds (Timireva and Velichko, 2006). This suggestion is supported by the dominance of sedimentary structures attributed to a low-speeded (up to 6 m/s) agent (Zieliński and Issmer, 2008). In contrast, a rather high frequency of RM grains is noted in areas with a significant duration of aeolian activity, such as in central Poland (Cailleux, 1942; Goździk, 2007); we deduce that the increase in number of RM grains seems to be unusual in Estonian localities. The cause of this remains unexplained, although this pattern might originate from the older (pre-Quaternary) deposits since they are spatially close. This suggestion relies on Kleesment (2009) and Mahaney and Kalm (2000); they found over 50% of rounded and subrounded quartz grains within Devonian sandstones. Late Weichselian tills contain over 15% of grains with completely preserved pre-glacial surface characteristics (Mahaney and Kalm, 2000).

Angular grains are usually connected with a glacial environment where they are crushed, or high-energetic subaqueous environments with limited transport distances, causing grain breakage without edge rounding (Helland and Diffendal, 1997; Helland and Holmes, 1997; Immonen, 2013). In contrast, angular outlines are rather rare in the aeolian environment (Vos et al., 2014). However, Bull and Morgan (2007) have distinguished angular aeolian-type grains with upturned plates from those without upturned plates, but with indentations. A similar approach was tested by Kalińska and Nartišs (2014). Abundant NU/M quartz grains may be characterised by two features: (1) their angularity and sharp edges, and (2) their specific surface area; under a binocular microscope this resembles frosting. An uneven shell-like surface of quartz grains is caused by the splitting by seasonal freezing of fluids; this is frequently observed within palaeosols of loess sequences (Velichko and Timirieva, 1995). We conclude that the transforming process arose as a consequence of strong chemical and/or mechanical weathering *in situ*; as a result, no traces of transportation can be found (Sokołowski et al., 2014). Similarly, the high content of cracked (C) grains probably results from post-sedimentary frost weathering (Woronko and Hoch, 2011; Woronko, 2012a). A high content of this grain type has been reported from former periglacial areas such as north-eastern Poland (Woronko et al., 2013), and is thought to indicate the relatively high moisture of the windblown sediments (Woronko and Pochocka-Szwarc, 2013).

The great variability of quartz grains forming the dunes of the Iisaku area is more characteristic of a glaciofluvial environment than an aeolian one. The morphology of landforms (parabolic dunes) and the sedimentary record (i.e. low-angle cross-stratification) point to a dune-like environment, whereas the transportation record reflects short term and/or short distance transport, and the contribution of neighbouring sedimentary environments.

Quartz and feldspar-rich sediments are the most extensive dune-forming sediments worldwide (Muhs, 2004). The quartz contents of selected areas of Australia (Goudie et al., 1993), North America (Billingsley, 1987) or central Poland (Mycielska-Dowgiałło, 1993) are generally over 90%. Feldspar is less durable than quartz, both during mechanical abrasion and chemical weathering (Pye and Tsoar, 2009), and so the dominance of the highly mechanically-resistant quartz points to multiple reworking and abrasion (Mycielska-Dowgiałło and Woronko, 2004). The mineralogical maturity is achieved not from extended periods of stability and weathering, but also from extended periods of aeolian activity (Muhs, 2004). The mixture of quartz grain types (representing various sedimentary environments but dominated by aeolian transport and deposition), as well as the relatively large amount of feldspar, suggest that the source was from some combination of igneous rocks. The Iisaku aeolian composition shows a similar trend to the channel-filling glaciofluvial material of the Iisaku morainic ridge, and we deduce that the quartz in these sediments has a similar provenance. The textural properties of the aeolian deposits

in Iisaku and surrounding environments are also very similar, suggesting a local origin.

6.2. Age estimates interpreted in a palaeogeographic and -climatic context

Seven, relatively closely-spaced quartz luminescence ages were obtained from the aeolian sequence in Iisaku, allowing us to establish an independent chronological framework covering the Late-glacial–Holocene transition in this part of NE Estonia. The palaeogeography of this region was strongly controlled by the production of a large volume of meltwater in front of the retreating glacier (Vassiljev and Saarse, 2013). All luminescence results obtained correlate well with the stages of the Baltic Ice Lake (BIL) development in the area (Vassiljev and Saarse, 2013), with OSL ages of 13.3 ± 1.2, 12.5 ± 0.8–12.7 ± 0.8 and 10.5 ± 0.7–11.5 ± 0.7 ka; these ages coincide with the A_2, BI and BIII stages, respectively. Apart from the regional geological situation, a particular combination of circumstances is required to form and mobilise dunes: (1) aridity (2) a reduction of the amount of vegetation, (3) a change in the ratio of annual precipitation to potential evapotranspiration, and (4) an increase in the wind velocity (Swezey et al., 2013) – a threshold shear velocity of 20–40 cm/s sustains aeolian mobilisation of the 0.08–0.8 mm diameter grains (Chepil and Woodruff, 1963). Because of the need for these conditions, aeolian activity in this area only occurred after the Baltic Ice Lake retreat.

The oldest of the samples (13.3 ± 1.2 ka; Iisaku 2 profile) was collected from the sediments on the leeward slope. At 13.3 cal ka BP (Heinsalu and Veski, 2007), the entire area between the Last Glacial Maximum ice extent and the local present Baltic coastline was ice-free and large water bodies in front of the Scandinavian Ice Sheet encouraged a more rapid decay of the ice margin due to calving (Lasberg and Kalm, 2013). Textural analysis suggests a decreasing number of EM/RM and RM aeolian type grains. This is consistent with the smaller proportion of quartz (Table 2) indicating a lower mineralogical maturity. These characteristics can be explained by: (1) a poor (initial?) aeolian transformation, (2) the inheritance of potential source sediment features, e.g. moraine derived, glacio-fluvial and glacio-lacustrine, and (3) a predominance of strong chemical/mechanical weathering conditions without any significant effect of the transporting agent(s). In addition, no transformation resulting from fluvial transport or any other interaction with water has been found in the sedimentary record.

Studies of lakes located ~70 km northeast of the Iisaku sites close to the proximal belt of the Pandivere zone and showed sandy-silty and silty and clayey-silty accumulation at 13.3 cal ka BP (Saarse et al., 2012) in a glaciolacustrine sedimentary environment. However, the palaeogeographical reconstruction of BIL at about 13.3 ka suggests the existence of an island located north of Lake Peipsi and separating the latter from the BIL A_2 stage (Vassiljev and Saarse, 2013). The position of the lower shoreline narrowed the connection between Lake Peipsi basin and the BIL (Rosentau et al., 2007) increasing the size of the island. The luminescence age of the sample (sample 123071; Table 1) taken from the middle of the leeward slope could place the Iisaku area within this hypothesised island. This is in contrast to the latest modelling results suggesting the lowering of the lake water level by ~15 m in the east (Vassiljev and Saarse, 2013). This places the Iisaku 2 site under the water table based on its elevation with respect to lake level, and falls into the time range when the area should have been a strait-like connection between Lake Peipsi and the BIL. Nevertheless, there is no reason to question the OSL age of 13.3 ± 1.2 ka for this specific sample. Both the spread in equivalent doses and the overall behaviour is similar compared to the other samples. Given the uncertainties in the age estimates, the OSL age of this sample may document the beginning of aeolian activity at this location. At the same time, the horizontally and climbing translatent stratificated *(Src)* sands intercalated with silt or silty sands with wavy lamination *(SFh,w)* described in the lowermost part of the Iisaku 3 profile (but without a luminescence sample; Figs. 3B and 4) could point to a transition from a glacio-lacustrine to an aeolian depositional environment. This is supported by the larger number of shiny quartz grains found at the bottom of the profile. In summary, there is some evidence that this site reflects the initiation of aeolian activity, but more luminescence ages from this area are needed to confirm this conclusion.

The sediments in the Iisaku 1 profile were dated to between 12.8 ± 0.8 ka and 12.5 ± 0.8 ka, 11.5 ± 0.7 ka and 11.3 ± 0.7 ka, and 10.9 ± 0.8 ka and 10.5 ± 0.7 ka (Table 1), suggesting the possibility of three aeolian events. However, the presence of horizontal/wavy laminations (*Sh*) in the lowermost part of the profile might reflect a glaciolacustrine environment (Figs. 3B and 4). Four of the ages are indistinguishable. This may be due to a period of rapid deposition as also noted in Dutch aeolian sediments (Vandenberghe et al., 2013); a higher sampling resolution would resolve this.

Overall, the deposition of the oldest sediment sequence observed in Iisaku 1 profile coincides with the ice retreat from the Palivere zone at 12.7 ka (Kalm et al., 2011). New results (Saarse et al., 2012; Vassiljev and Saarse, 2013) suggest that the Palivere ice re-advance ceased in the Allerød chronozone. According to data from the Pääsküla site (Northern Estonia) the Palivere marginal zone formed prior to 13.3 cal. BP (Lasberg and Kalm, 2013). Thus the two optical ages of 12.8 ± 0.8 ka and 12.5 ± 0.8 ka (samples 123074 and 123076) may represent the 1300-year long Younger Dryas cold reversal (Fiedel, 2011). Although aeolian-transformed quartz grains dominate in the Iisaku 1 profile during that time period, their variability may reflect favourable conditions for accumulation. Aeolian deposition occurred most likely during winter when sand was freed from the frozen soil by sublimation or evaporation (McKenna Neuman, 2004). Given the textural features, parts of the profile with dominant aeolian-type grains may reflect winter conditions, whereas the *in situ* weathered grains point to a periglacial climate with seasonal freezing and thawing. Younger Dryas cooling is clearly documented in the neighbourhood of Lake Äntu Sinijärv (Laumets et al., 2014). There an abrupt change in pollen, typical of open Arctic environments, has been noted at 11,800–11,700 cal. BP, together with a mineral inflow layer within the thick gyttja sequence.

According to Sohar and Kalm (2008) the ostracode faunal assemblages from Lake Sinijärv indicate one of the major low-water periods, with fresh water tufa precipitation at 11,600–10,590 cal. BP triggered by the relatively high air temperature and increased evaporation. That period correlates with the last drainage event of the BIL at 11,650 cal yr BP (Vassiljev and Saarse, 2013). The luminescence ages from the Iisaku 1 profile of between 11.5 ± 0.7 and 10.9 ± 0.8 ka indicate that aeolian deposition continued across the Younger Dryas/Holocene boundary (11,700 calendar years b2k; Walker et al., 2009). The alternating decrease and increase in aeolian-type grains may reflect seasonally varying (from weaker to stronger) aeolian activity. This combination, together with the sedimentary structures and geomorphology, suggest the existence of areas with discontinuous vegetation, allowing grain mobilisation by wind.

The massive sands deposited in the uppermost part of the Iisaku 1 profile give an age of 10.5 ± 0.7 ka. This deposition seems to be climatically controlled by the first post-glacial transgression noted in the small lowland lakes in Estonia, reflecting a change from a warm-to cold-temperature ostracode assemblage at 10,590 cal. BP (Sohar and Kalm, 2008). The early Holocene aeolian activity built drift-like forms blanketing the pre-existing dunes and seems to have been continuous since the Late-glacial, as no hiatuses, organic and loamy bed or other sediment transition have been noted. A similar Late-glacial–Holocene transition has been reported from northwestern Europe (Kolstrup, 2007).

7. Conclusions

A new set of luminescence ages has been presented for an aeolian inland dune complex (Iisaku sites), NE Estonia; these show the sediment was deposited during the Last-glacial/Holocene transition. By considering these ages together with the unusual structural and textural properties of these aeolian sediments, the palaeoenvironmental history of the region has been reconstructed.

Quartz grains of the 0.5–0.8 and 0.8–1.0 mm sand fractions recorded the dominant aeolian conditions. At the same time strong chemical/mechanical weathering processes also affected the timing of dune formation. Overall, the textural characterisation suggests short-duration transportation or/and short transport distance and a contribution from neighbouring sedimentary environments.

The dune development in the area was strongly controlled by the formation of the Baltic Ice Lake (BIL) in front of the retreating glacier. The luminescence ages of the aeolian complex represent a continuous time span between 13.3 ± 1.2 to 10.5 ± 0.7 ka. Similar phenomena have been observed only in a few European localities, making this site rather unique. Four partially overlapping phases of aeolian activity may be documented: (1) a phase at 13.3 ± 1.2 ka which most likely can be correlated with the existence of an island separating the BIL and Lake Peipsi, (2) a sedimentologically-distinct phase around 12.7 ± 0.8 ka and 12.5 ± 0.8 ka, presumably representing the Younger Dryas cold reversal, clearly recorded in the sediments of the neighbourhood Lake Äntu Sinijärv, (3) a phase between 11.5 ± 0.7 ka and 10.9 ± 0.8 ka correlated with the last drainage event of the BIL at 11,650 cal. BP, and (4) a phase correlated with the first post–glacial transgression previously noted in small lowland lakes in Estonia and reflected by sand-drift (although this phase is only documented by a single age of 10.5 ± 0.7 ka). Although it is acknowledged that the luminescence ages from sedimentologically distinct units overlap within errors, the new luminescence chronology clearly challenges the previous assumption of exclusively Holocene ages of the Iisaku inland dunes. The origins of the discrepancy of our ages compared to the previous study needs to be resolved.

Acknowledgments

The authors wish to thank Dr. Katrin Lasberg (University of Tartu) and Alexander Gorlach (University of Tartu) for their help during fieldwork. We thank to Prof. Vitālijs Zelčs (University of Latvia) for his support and anonymous reviewers for constructive comments. The study was funded by the Postdoctoral Research Grant ERMOS (22) (FP7 Marie Curie Cofund the “People” programme) “Age and climatic signature of coversands deposits distributed on glaciolacustrine basins along the Scandinavian Ice Sheet margin southeast of the Baltic Sea”.

References

Amon, L., Veski, S., Heinsalu, A., Saarse, L., 2012. Timing of Lateglacial vegetation dynamics and respective palaeoenvironmental conditions in southern Estonia: evidence from the sediment record of Lake Nakri. Journal of Quaternary Science 27, 169–180.

Bateman, M.D., Van Huissteden, J., 1999. The timing of last-glacial periglacial and aeolian events, Twente, eastern Netherlands. Journal of Quaternary Sciences 14, 277–283.

Billingsley, G.H., 1987. Geology and Geomorphology of the Southwestern Moenkopi Plateau and Southern Ward Terrace, Arizona. U.S. G.P.O, Washington and Denver, CO.

Bull, P.A., Morgan, R.M., 2007. Sediment fingerprints: a forensic technique using quartz sand grains. Science & Justice: Journal of the Forensic Science Society 47, 107–124.

Cailleux, A., 1942. Les actiones éoliennes périglaciaires en Europe. In: Mémoires de la Société Géologique de France, vol. 41, pp. 1–176.

Cailleux, A., 1952. Morphoskopische Analyse der Geschiebe und Sandkörner und Ihre Bedeutung für die Paläoklimatologie. Geologische Rundau 40, 11–19.

Chepil, W.S., Woodruff, N.P., 1963. The physics of wind erosion and its control. In: Norman, A.G. (Ed.), Advances in Agronomy. Academic Press, New York, pp. 211–302.

Denby, P.M., Bøtter-Jensen, L., Murray, A.S., Thomsen, K.J., Moska, P., 2006. Application of pulsed OSL to the separation of the luminescence components from a mixed quartz/feldspar sample. Radiation Measurements 41, 774–779.

Derese, C., Vandenberghe, D., Paulissen, E., Van den Haute, P., 2009. Revisiting a type locality for Late Glacial aeolian sand deposition in NW Europe: optical dating of the dune complex at Opgrimbie (NE Belgium). Geomorphology 109, 27–35.

Duller, G.A.T., 2003. Distinguishing quartz and feldspar in single grain luminescence measurements. Radiation Measurements 37, 161–165.

Estonian Land Board, 2013. Grayscale Hillshading Based on Lidar Elevation Data ([WWW Document]. Public WMS-service).

Fiedel, S.J., 2011. The mysterious onset of the Younger Dryas. Quaternary International 242, 262–266.

Folk, R.L., Ward, W.C., 1957. Brazos River Bar: a study in the significance of grain size parameters. Journal of Sedimentary Petrology 27, 3–26.

Gilbert, E.R., De Camargo, M.G., Sandrini-Neto, L., 2012. Rysgran: Grain Size Analysis, Textural Classifications and Distribution of Unconsolidated Sediments.

Goudie, A.S., Stokes, S., Livingstone, I., Bailiff, I.K., Allison, R.J., 1993. Post-Depositional modification of the linear sand ridges of the west Kimberley area of North-West Australia. The Geographical Journal 159, 306–317.

Goździk, J., 2007. The Vistulian aeolian succession in central Poland. Sedimentary Geology 193, 211–220.

Hang, T., 2003. A local clay-varve chronology and proglacial sedimentary environment in glacial Lake Peipsi, eastern Estonia. Boreas 32, 416–426.

Hang, T., Kohv, M., 2013. Glacial varves at Pärnu, south-western Estonia: a local varve chronology and proglacial sedimentary environment. GFF 135, 273–281.

Hang, T., Ojala, A., Kohv, M., Tuvikene, T., 2011. Varve chronology and proglacial sedimentary environment in Pärnu area, western Estonia. In: Johansson, P., Lunkka, J.P., Sarala, P. (Eds.), Late Pleistocene Glacigenic Deposits from the Central Part of the Scandinavian Ice Sheet to Younger Dryas End Moraine Zone. Geological Survey of Finland, Rovaniemi, pp. 94–95.

Hanson, M.A., Lian, O.B., Clague, J.J., 2012. The sequence and timing of large late Pleistocene floods from glacial Lake Missoula. Quaternary Science Reviews 31, 67–81.

Heinsalu, A., Veski, S., 2007. The history of the Yoldia Sea in Northern Estonia: palaeoenvironmental conditions and climatic oscillations. Geological Quarterly 51, 295–306.

Helland, P.E., Diffendal, R.F., 1997. SEM analysis of quartz sand grain surface textures indicates alluvial/colluvial origin of the Quaternary “Glacial”Boulder Clays at Huangshan (Yellow Mountain), East-Central China. Quaternary Research 48, 177–186.

Helland, P.E., Holmes, M.A., 1997. Surface textural analysis of quartz sand grains from ODP Site 918 off the southeast coast of Greenland suggests glaciation of southern Greenland at 11 Ma. Palaeogeography, Palaeoclimatology, Palaeoecology 135, 109–121.

Immonen, N., 2013. Surface microtextures of ice-rafted quartz grains revealing glacial ice in the Cenozoic Arctic. Palaeogeography, Palaeoclimatology, Palaeoecology 374, 293–302.

Jankowski, M., 2012. Lateglacial soil paleocatena in inland-dune area of the Toruń Basin, Northern Poland. Quaternary International 265, 116–125.

Kaiser, K., Hilgers, A., Schlaak, N., Jankowski, M., Kühn, P., Bussemer, S., Przegiętka, K., 2009. Palaeopedological marker horizons in northern central Europe: characteristics of Lateglacial Usselo and Finow soils. Boreas 38, 591–609.

Kalińska, E., 2012. Geological setting and sedimentary characteristics of the coversands distributed in the western part of the Blonie glaciolacustrine basin (Central Poland) – preliminary results. Bulletin of the Geological Society of Finland 84, 33–44.

Kalińska, E., Nartišs, M., 2014. Pleistocene and Holocene aeolian sediments of different location and geological history: a new insight from rounding and frosting of quartz grains. Quaternary International 328-329, 311–322.

Kalm, V., 2006. Pleistocene chronostratigraphy in Estonia, southeastern sector of the Scandinavian glaciation. Quaternary Science Reviews 25, 960–975.

Kalm, V., Raukas, A., Rattas, M., Lasberg, K., 2011. Pleistocene glaciations in Estonia. In: Ehlers, J., Gibbard, P.L., Hughes, P.D. (Eds.), Quaternary Glaciations – Extent and Chronology, Developments in Quaternary Science. Elsevier Inc., Amsterdam, pp. 95–104.

Kasse, C., 1997. Cold-climate aeolian sand-sheet formation in North-Western Europe (c. 14-12.4 ka); a response to permafrost degradation and increased aridity. Permafrost and Periglacial Processes 8, 295–311.

Kasse, C., 2002. Sandy aeolian deposits and environments and their relation to climate during the Last Glacial Maximum and Lateglacial in northwest and central Europe. Progress in Physical Geography 26, 507–532.

Kasse, C., Vandenberghe, D., De Corte, F., Van Den Haute, P., 2007. Late Weichselian fluvio-aeolian sands and coversands of the type locality Grubbenvorst (southern Netherlands): sedimentary environments, climate record and age, vol. 22, pp. 695–708.

Kihno, K., Saarse, L., Amon, L., 2011. Late Glacial vegetation, sedimentation and ice recession chronology in the surroundings of Lake Prossa, central Estonia. Estonian Journal of Earth Sciences 60, 147–158.

Kleesment, A., 2009. Roundness and surface features of quartz grains in Middle Devonian deposits of the East Baltic and their palaeogeographical implications. Estonian Journal of Earth Sciences 58, 71.

Kolstrup, E., 2007. Lateglacial older and younger coversand in northwest Europe: chronology and relation to climate and vegetation. Boreas 36, 65–75.
Konecka-Betley, K., Janowska, E., 1976. Late Glacial and Holocene stratotipe profile of palaeosoils in the Warsaw Basin. Studia Quaternaria 22, 3–16.
Koster, E.A., 2005. Recent advances in luminescence dating of Late Pleistocene (cold-climate) aeolian sand and loess deposits in western Europe. Permafrost and Periglacial Processes 16, 131–143.
Kotilainen, M., 2004. Dune stratigraphy as an indicator of Holocene climatic change and human impact in Northern Lapland, Finland. Annales Academiae Scientiarum Fennicae, Geologica-Geographica 166, 1–158.
Krumbein, W.C., 1941. Measurement and geological significance of shape and roundness of sedimentary particles. Journal of Sedimentary Research 11, 64–72.
Lasberg, K., Kalm, V., 2013. Chronology of Late Weichselian glaciation in the western part of the East European Plain. Boreas 42, 995–1007.
Laumets, L., Kalm, V., Poska, A., Kele, S., Lasberg, K., Amon, L., 2014. Palaeoclimate inferred from $\delta^{18}O$ and palaeobotanical indicators in freshwater tufa of Lake Äntu Sinijärv, Estonia. Journal of Paleolimnology 51, 99–111.
Mahaney, W.C., Kalm, V., 2000. Comparative scanning electron microscopy study of oriented till blocks, glacial grains and Devonian sands in Estonia and Latvia. Boreas 29, 35–51.
Mardla, E.E., 1967. The Geological Map of USSR (Quaternary Deposits) 1:200 000, O-35-IV Sheet. Moscow.
McKenna Neuman, C., 2004. Effects of temperature and humidity upon the transport of sedimentary particles by wind. Sedimentology 51, 1–17.
Miall, A.D., 1977. Lithofacies types and vertical profile models in braided river deposits: a summary. Fluvial Sedimentology 5, 597–604.
Miall, A.D., 1978. Lithofacies types and vertical profile models in braided river deposits: a summary. In: Miall, A.D. (Ed.), Fluvial Sedimentology. Can. Soc. Petrol. Geol. Mem, pp. 597–604.
Muhs, D.R., 2004. Mineralogical maturity in dunefields of North America, Africa and Australia. Geomorphology 59, 247–269.
Murray, A.S., Marten, R., Johnston, A., Martin, P., 1987. Analysis for naturally occuring radionuclides at environmental concentrations by gamma spectrometry. Journal of Radioanalytical and Nuclear Chemistry 115, 263–288.
Murray, A.S., Wintle, A.G., 2000. Luminescence dating of quartz using an improved single-aliquot regenerative-dose protocol. Radiation Measurements 32, 57–73.
Mycielska-Dowgiałło, E., 1993. Estimates of late glacial and holocene aeolian activity in Belgium, Poland and Sweden. Boreas 22, 165–170.
Mycielska-Dowgiałło, E., 2007. Metody badań cech teksturalnych osadów klastycznych i wartość interpretacyjna wyników. In: Mycielska-Dowgiałło, Elżbieta, Rutkowski, J. (Eds.), Badania Cech Teksturalnych Osadów Czwartorzędowych I Wybrane Metody Oznaczania Ich Wieku. WSWPR, pp. 95–189.
Mycielska-Dowgiałło, E., Dzierwa, K., 2003. Rekonstrucja dynamiki procesów eolicznych i czasu ich trwania na podstawie wybranych cech teksturalnych osadów wydmy w Cięciwie. Przegląd Geologiczny 51, 163–167.
Mycielska-Dowgiałło, E., Woronko, B., 2004. The degree of aeolization of Quaternary deposits in Poland as a tool for stratigraphic interpretation. Sedimentary Geology 168, 149–163.
Mycielska-Dowgiałło, E., Woronko, B., 1998. Analiza obtoczenia i zmatowienia powierzchni ziarn kwarcowych frakcji piaszczystej i jej wartość interpretacyjna. Przegląd Geologiczny 46, 1275–1281.
Narayana, A.C., Mohan, R., Mishra, R., 2010. Morphology and surface textures of quartz grains from freshwater lakes of McLeod Island, Larsemann Hills, East Antarctica. Current Science 99, 1420–1424.
Olley, J.M., Murray, A.S., Roberts, R.G., 1996. The effects of disequilibria in the uranium and thorium decay chains on burial dose rates in fluvial sediments. Quaternary Science Reviews 15, 751–760.
Pernarowski, L., 1962. O procesach wydmotwórczych. Czasopismo Geograficzne 33, 173–197.
Pye, K., Tsoar, H., 2009. Aeolian Sand and Sand Dunes. Springer-Verlag Berlin Heidelberg, Lepizig.
Rasmussen, S.O., Andersen, K.K., Svensson, A.M., Steffensen, J.P., Vinther, B.M., Clausen, H.B., Siggaard-Andersen, M.-L., Johnsen, S.J., Larsen, L.B., Dahl-Jensen, D., Bigler, M., Röthlisberger, R., Fischer, H., Goto-Azuma, K., Hansson, M.E., Ruth, U., 2006. A new Greenland ice core chronology for the last glacial termination. Journal of Geophysical Research: Atmospheres 111, 1–16.
Raukas, A., 1999. Aeolian activity. In: Miidel, Avo, Raukas, Anto (Eds.), Lake Peipsi. Geology. Sulemees Publishers, Tallinn, pp. 120–124.
Raukas, A., 2011. Evolution of aeolian landscapes in north-eastern Estonia under environmental changes. Geographia Polonica 84, 117–126.
Raukas, A., Hüüt, G., 1988. On the luminescence dating of aeolian deposits in Estonia. Baltica 11, 17–24.
Rinterknecht, V.R., Clark, P.U., Raisbeck, G.M., Yiou, F., Bitinas, A., Brook, E.J., Marks, L., Zelcs, V., Lunkka, J.-P., Pavlovskaya, I.E., Piotrowski, J.A., Raukas, A., 2006. The last deglaciation of the southeastern sector of the Scandinavian ice sheet. Science (New York, N.Y 311, 1449–1452.
Ritchot, G., Cailleux, A., 1971. Taxonomie, géomorphologie et morphoscopie de sables au Québec méridional. Cahiers de géographie du Québec 15, 423.
Rosentau, A., Vassiljev, J., Saarse, L., Miidel, A., 2007. Palaeogeographic reconstruction of proglacial lakes in Estonia. Boreas 36, 211–221.
Saarnisto, M., Saarinen, T., 2001. Deglaciation chronology of the scandinavian ice sheet from the Lake Onega Basin to the Salpausselkä end moraines. Global and Planetary Change 31, 387–405.
Saarse, L., Heinsalu, A., Veski, S., 2012. Deglaciation chronology of the Pandivere and Palivere ice-marginal zones in Estonia. Geological Quarterly 56, 353–362.
Sohar, K., Kalm, V., 2008. A 12.8-ka-long palaeoenvironmental record revealed by subfossil ostracod data from lacustrine freshwater tufa in Lake Sinijärv, northern Estonia. Journal of Paleolimnology 40, 809–821.
Sokołowski, T., Wacnik, A., Woronko, B., Madeja, J., 2014. Eemian Weichselian Pleniglacial fluvial deposits in S Poland (an example of the Vistula River valley in Kraków). Geological Quarterly 58, 71–84.
Swezey, C.S., Schultz, A.P., González, W.A., Bernhardt, C.E., Doar, W.R., Garrity, C.P., Mahan, S.A., McGeehin, J.P., 2013. Quaternary eolian dunes in the Savannah River valley, Jasper County, South Carolina, USA. Quaternary Research 80, 250–264.
Syvitski, J.P.M., 1991. Principles, Methods, and Application of Particle Size Analysis. Cambridge University Press, Cambridge.
Talviste, P., Hang, T., Kohv, M., 2012. Glacial varves at the distal slope of Pandivere – Neva ice-recessional formations in western Estonia. Bulletin of the Geological Society of Finland 84, 7–19.
Thomsen, K.J., Bøtter-Jensen, L., Denby, P.M., Moska, P., Murray, A.S., 2006. Developments in luminescence measurement techniques. Radiation Measurements 41, 768–773.
Thomsen, K.J., Jain, M., Murray, a. S., Denby, P.M., Roy, N., Bøtter-Jensen, L., 2008. Minimizing feldspar OSL contamination in quartz UV-OSL using pulsed blue stimulation. Radiation Measurements 43, 752–757.
Timireva, S.N., Velichko, a. a, 2006. Depositional environments of the Pleistocene loess-soil series inferred from sand grain morphoscopy—A case study of the East European Plain. Quaternary International 152-153, 136–145.
Vandenberghe, D.A.G., Derese, C., Kasse, C., Van den Haute, P., 2013. Late Weichselian (fluvio-)aeolian sediments and Holocene drift-sands of the classic type locality in Twente (E Netherlands): a high-resolution dating study using optically stimulated luminescence. Quaternary Science Reviews 68, 96–113.
Vassiljev, J., Saarse, L., 2013. Timing of the Baltic Ice Lake in the eastern Baltic. Bulletin of the Geological Society of Finland 85, 9–18.
Velichko, A.A., Timireva, S.N., Kremenetski, K.V., MacDonald, G.M., Smith, L.C., 2011. West Siberian Plain as a late glacial desert. Quaternary International 237, 45–53.
Velichko, A.A., Timirieva, S.N., 1995. Morphoscopy and Morphometry of quartz grains from loess and Buried soil layers. GeoJournal 36, 143–149.
Veski, S., Amon, L., Heinsalu, A., Reitalu, T., Saarse, L., Stivrins, N., Vassiljev, J., 2012. Lateglacial vegetation dynamics in the eastern Baltic region between 14,500 and 11,400calyrBP: a complete record since the Bølling (GI-1e) to the Holocene. Quaternary Science Reviews 40, 39–53.
Vos, K., Vandenberghe, N., Elsen, J., 2014. Surface textural analysis of quartz grains by scanning electron microscopy (SEM): from sample preparation to environmental interpretation. Earth-Science Reviews 128, 93–104.
Walker, M., Johnsen, S., Rasmussen, S.O., Popp, T., Steffensen, J., Cwynar, L.E.S.C., Hughen, K., Gibbard, P., Hoek, W.I.M., Lowe, J., Andrews, J., Bjo, S., 2009. Formal definition and dating of the GSSP (Global Stratotype Section and Point) for the base of the Holocene using the Greenland NGRIP ice core, and selected auxiliary records. Journal of Quaternary Science 24, 3–17.
Wintle, A.G., Murray, A.S., 2006. A review of quartz optically stimulated luminescence characteristics and their relevance in single-aliquot regeneration dating protocols. Radiation Measurements 41, 369–391.
Woronko, B., 2012a. Zapis procesów eolicznych w osadach piaszczystych plejstocenu na wybranych obszarach Polski Środkowej i Północno-Wschodniej. Wydział Geografii i Studiów Regionalnych, Uniwersytet Warszawski, Warszawa.
Woronko, B., 2012b. Micromorphology of quartz grains as a tool in the reconstruction of periglacial environment. In: Churski, P. (Ed.), Contemporary Issues in Polish Geography, pp. 111–131.
Woronko, B., Hoch, M., 2011. The development of frost-weathering microstructures on sand-sized quartz grains: examples from Poland and Mongolia. Permafrost and Periglacial Processes 227, 214–227.
Woronko, B., Pochocka-Szwarc, K., 2013. Depositional environment of a fan delta in a Vistulian proglacial lake (Skaliska Basin, north-eastern Poland). Acta Palaeobotanica 53, 9–21.
Woronko, B., Rychel, J., Karasiewicz, M.T., Ber, A., Krzywicki, T., Marks, L., Pochocka-Szwarc, K., 2013. Heavy and light minerals as a tool for reconstructing depositional environments: an example from the Jałówka site (northern Podlasie region, NE Poland). Geologos 19, 47–66.
Zeeberg, J., 1998. The European sand belt in eastern Europe – and comparison of Late Glacial dune orientation with GCM simulation results. Boreas 27, 127–139.
Zieliński, P., Issmer, K., 2008. Propozycja kodu genetycznego osadów środowiska eolicznego. Przegląd Geologiczny 56, 67–72.
Zieliński, P., Sokołowski, R.J., Fedorowicz, S., Zaleski, I., 2014. Periglacial structures within fluvio-aeolian successions of the end of the Last Glaciation – examples from SE Poland and NW Ukraine. Boreas 43, 712–721.
Zieliński, T., Pisarska-Jamroży, M., 2012. Jakie cechy litologiczne osadów warto kodować, a jakie nie? Przegląd Geologiczny 60, 387–397.